Reducing the number of computations in stack decoding of convolutional codes by exploiting symmetries of the encoder

th e

Reducing the number of computations in stack decoding of convolutional codes by exploiting symmetries of the encoder

by

A.J.. Vinck and A.J.P. de Paepe

E I N D H O V E N U N I V E R S I T Y O F T E C H N O L O G Y
Department of Electrical Engineering
Eindhoven The Netherlands

REDUCING THE NUMBER OF COMPUTATIONS IN STACK DECODING OF CONVOLUTIONAL CODES BY EXPLOITING SYMMETRIES OF THE ENCODER.

by

A.J. Vinck
and
A.J.P. de Paepe

TH-Report 78-E-90
ISBN 90-6144-090-4

Eindhoven
September 1978

CONTENTS

Abstract

This report describes a method of decoding of convolutional codes, where the decoding algorithm looks for an information-vector correction sequence, that must be added to the inverse of the received data vector sequence. This in contrast with the usual method, that tries to estimate the information vector sequence directly. Both methods are equally complex for a maximum likelihood (ML) decoder. In sequential decoding, with hard as well as with soft decisions, symmetries of the code can be exploited to reduce the number of computations and hence, the erasure probability. This will be illustrated by simulation results. The method is related to [1,2,3], where Schalkwijk et al. use state space symmetries of the syndrome former to obtain a reduction in the exponential rate of growth of the hardware of a Viterbi-like syndrome decoder.

This research was partly supported by the Netherlands Organization for the Advancement of Pure Research (Z.W.O.).

Introduction

We first describe the general concept of convolutional encoding. Some of the results of [4] are reviewed, and extended where necessary.

A binary convolutional encoder G is a linear sequential machine with k binary inputs and n binary outputs. The input-output relation can be described, Forney [4], by a kxn polynomial generator matrix G as

$$\underline{T}(D) = \underline{I}(D)G \ ,$$

where

$$\underline{I}(D) = (I^1(D) \ , I^2(D) \ , \ \ldots \ , \ I^k(D)) \ , \text{ and}$$

$$\underline{T}(D) = (T^1(D) \ , T^2(D) \ , \ \ldots \ , \ T^n(D)) \ .$$

For notational convenience, we shall generally suppress the parenthetical D in our subsequent references to sequences. We first introduce some definitions that are usefull in the sequel.

Definition: A realization of an encoder with as much shift registers as inputs, is called obvious. If the number of shift registers is equal to the number of outputs, the realization is called adjoint obvious.

Definition: The physical state of a realization is equal to the contents of the memory elements of this realization.

Definition: The abstract state of a realization is equal to the output of a realization under a sequence of all zero input vectors.

It can be proven, Forney [4], that for a minimal (minimal number of memory elements) realization the number of abstract states equals the number of physical states, and that they are uniquely related. Note that in the adjoint obvious realization the physical state equals the abstract state. If we define the constraint length for the i-th input as

$$\nu_i = \max_{1 \leq j \leq n} \left[\deg G^{ij} \right] ,$$

then the overall constraint length

$$\nu = \sum_{i=1}^{k} \nu_i ,$$

equals the number of memory elements for the obvious realization of the encoder. G is called basic, if it has a feedback-free inverse G^{-1}, i.e. G^{-1} is polynomial and $G\, G^{-1} = I_k$. A basic encoder G is minimal if its overall constraint length ν in the obvious realization equals the maximum degree μ of its kxk sub-determinants. For more details about the above definitions and their consequences, see [4].

The dual code $C^{\perp}$ to a convolutional code C, generated by an encoder G, is the linear space generated by the set of all n-tuples of finite sequences $\underline{Y}$, such that the inner product $(\underline{X},\underline{Y}) \triangleq \underline{X}.\underline{Y}^T$ (where T means transpose) is zero for all $\underline{X}$ in C. The dual code of a rate k/n convolutional code may be generated by any rate (n-k)/n encoder H such that $G\, H^T = 0$. The n-input, (n-k)-output linear sequential circuit whose transfer function matrix is H^T, is called a syndrome former, and has the property that $\underline{X}\, H^T = \underline{0}$ iff $\underline{X} \in C$.

It can be shown, Forney [6], that when G and H are dual minimal encoders, an inverse encoder G^{-1} can be derived from the syndrome former H^T

without using additional memory elements. Furthermore, as H is minimal, also a feedback-free inverse H^{-1} exists, in the same sense as defined before. For example, Fig. 1 illustrates the obvious realization of the encoder

$$G = \begin{bmatrix} 1 & 1+D & D \\ 1+D^2 & D & 1 \end{bmatrix} , \tag{1}$$

with overall constraint length 3. For this encoder, the dual minimal encoder H

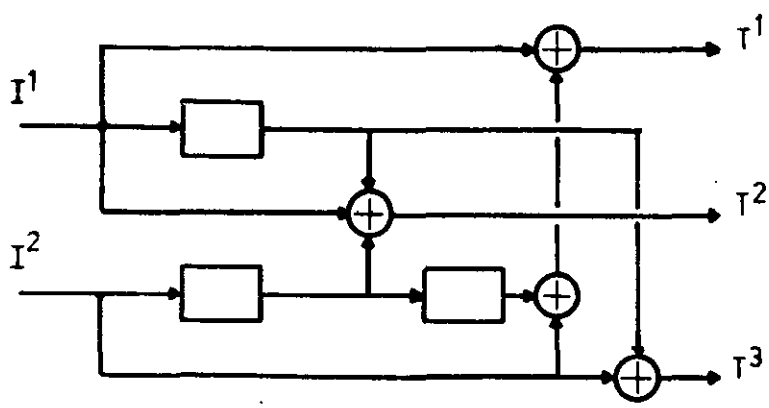

Fig. 1. Obvious realization of encoder G in (1).

and the inverses G^{-1} and H^{-1} are given below.

$$H = \begin{bmatrix} 1+D+D^2 & 1+D+D^3 & 1+D^2+D^3 \end{bmatrix} ,$$

$$G^{-1} = \begin{bmatrix} 1+D & 1 \\ D^2 & 1+D \\ 1+D+D^2 & D \end{bmatrix} , \qquad H^{-1} = \begin{bmatrix} D^2 \\ 1+D \\ 0 \end{bmatrix} . \tag{2}$$

The adjoint obvious realization of H^T is given in Fig. 2.

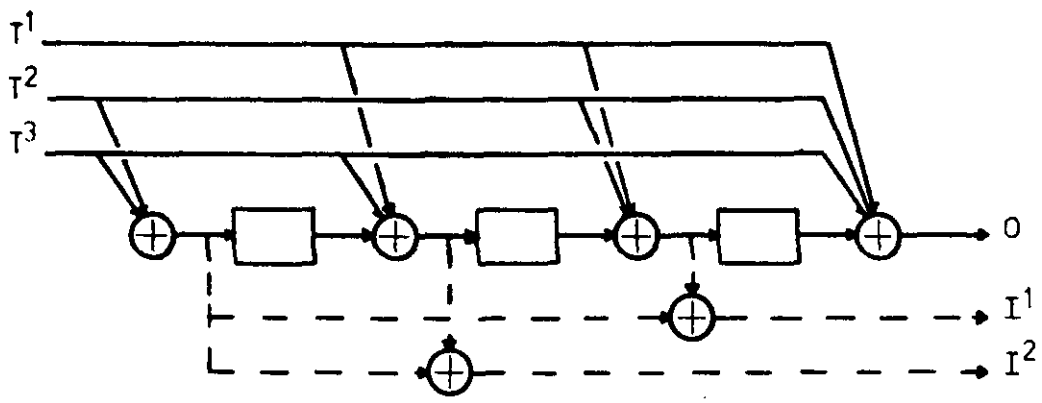

Fig. 2. Adjoint obvious realization of H^T in (2), and an inverse G^{-1}.

The polynomial matrices G, G^{-1}, H and H^{-1} can be combined in two square nxn matrices $[G^{-1}\ H^T]$ and $\begin{bmatrix} G \\ H^{-1^T} \end{bmatrix}$. The product of these matrices

$$\left[\begin{array}{c:c} G & \\ \hdashline & H^{-1^T} \end{array}\right] \left[\begin{array}{c:c} & H^T \\ \hdashline G & \end{array}\right] = \left[\begin{array}{c:c} G\,G^{-1} & G\,H^T \\ \hdashline H^{-1^T}\,G^{-1} & H^{-1^T}\,H^T \end{array}\right]$$

$$= \left[\begin{array}{c:c} I_k & 0_{k,n-k} \\ \hdashline H^{-1^T}\,G^{-1} & I_{n-k} \end{array}\right], \qquad (3)$$

and is equal to $[I_n]$, if $[H^{-1^T}\ G^{-1}] = [0_{n-k,k}]$. This can be accomplished by substituting H^{-1^T} by

$$\tilde{H}^{-1^T} = H^{-1^T} + H^{-1^T}\,G^{-1}\,G \quad ,$$

or G^{-1} by

$$\tilde{G}^{-1} = G^{-1} + H^T H^{-1^T} G^{-1} \quad .$$

Hence, given the encoder G, the dual encoder H and the corresponding inverse G^{-1}, a polynomial inverse matrix $\begin{bmatrix} G \\ H^{-1^T} \end{bmatrix}$ to $[G^{-1} \; H^T]$ can be derived. It will be this inverse matrix that plays the key role in the decoding procedure of the next section.

Decoding

We will now describe the use of the polynomial matrix $[G^{-1} \; H^T]$ and its inverse at the receiver, in order to decode a binary convolutional code. Assume that transmission of the code sequence $\underline{I}\,G$ is to be done over a binary symmetric channel (BSC). The received data vector sequence can be considered as a binary n-vector sequence $\underline{R} = \underline{I}\,G + \underline{N}$, where $\underline{N}$ represents the error vector sequence. We define the syndrome vector sequence $\underline{Z}$ as

$$\begin{aligned} \underline{Z} &\triangleq \underline{R}\,H^T \\ &= (\underline{I}\,G + \underline{N})\,H^T = \underline{N}\,H^T \quad , \end{aligned} \tag{4}$$

and the inverse to the received data vector sequence as

$$\begin{aligned} \underline{I} + \underline{E} &\triangleq \underline{R}\,G^{-1} \\ &= (\underline{I}\,G + \underline{N})\,G^{-1} = \underline{I} + \underline{N}\,G^{-1} \quad . \end{aligned} \tag{5}$$

The task of the ML decoder is to find an error vector sequence estimate $\hat{\underline{N}}$ of minimum Hamming weight that may be a possible cause of the syndrome vector sequence $\underline{Z}$. The inverse to this estimate, defined as

$$\hat{\underline{E}} \triangleq \hat{\underline{N}}\,G^{-1} \quad ,$$

must be added to $(\underline{I} + \underline{E})$, to give an estimate of the information vector sequence. Combining (4) and (5), we have

$$(\underline{I}\,G + \underline{N})\,[G^{-1} \; H^T] \triangleq (\underline{I} + \underline{E} \; , \; \underline{Z}) \quad , \tag{6}$$

or as the code vector sequence $\underline{I}\,G$ does not influence $\underline{E}$ and $\underline{Z}$,

$$\underline{N}\,[G^{-1}\ H^{T}] \triangleq (\underline{E},\underline{Z}) \quad . \tag{7}$$

For the estimate $\hat{\underline{N}}$, (7) becomes

$$\hat{\underline{N}}\,[G^{-1}\ H^{T}] \triangleq (\hat{\underline{E}},\underline{Z}) \quad . \tag{8}$$

The inverse $\begin{bmatrix} G \\ H^{-1^{T}} \end{bmatrix}$ to $[G^{-1}\ H^{T}]$ can now be used to rewrite (8) as

$$\begin{aligned} \hat{\underline{N}} &= (\hat{\underline{E}},\underline{Z}) \begin{bmatrix} G \\ H^{-1^{T}} \end{bmatrix} \\ &= \hat{\underline{E}}\,G + \underline{Z}\,H^{-1^{T}} \quad . \end{aligned} \tag{9}$$

In view of (4) and (9), we can describe two maximum likelihood decoding schemes. The first one, [1,2,3], is based on the state space generated by the syndrome former H^{T}. A possible noise vector sequence estimate $\hat{\underline{N}}$ corresponds with a path through the trellis, [5], of H^{T}. The estimation algorithm is to find a path of smallest Hamming weight that may be a cause of $\underline{Z}$. The noise vector sequence estimate $\hat{\underline{N}}$ is added to the received data vector sequence and the resulting codeword vector sequence estimate is then inverted using G^{-1} to form the information vector sequence estimate

$$\begin{aligned} \hat{\underline{I}} &= (\underline{I}\,G + \underline{N} + \hat{\underline{N}})G^{-1} \\ &= \underline{I} + (\underline{N} + \hat{\underline{N}})G^{-1} \quad . \end{aligned}$$

The complexity of this algorithm is strongly related to the size of the abstract state space of H^{T}. However, if G is a minimal encoder with constraint length ν, the syndrome former H^{T} can be realized with the same number of memory elements, see [3,4]. Hence, as this decoding scheme requires 2^{ν} trellis states, it is of the same complexity as the classical Viterbi decoder. Schalkwijk et al [1,2,3],

describe the above decoding strategy in detail. They have also shown, that certain state space symmetries of H^T can be exploited to reduce the complexity (hardware) of the so called syndrome decoder.

Equation (9) allows another decoding algorithm based on the state space (physical) generated by the encoder G. Given $\underline{Z}$, and hence $\underline{Z}\, H^{-1^T}$, this decoder finds that information sequence correction estimate $\hat{\underline{E}}$, such that $\hat{\underline{N}}$ is of minimum Hamming weight. This is equivalent to finding a codeword vector sequence $\hat{\underline{E}}\, G$ closest to $\underline{Z}\, H^{-1^T}$ in Hamming distance. This sequence can then be added to the inverse of the received data vector sequence to form the information vector sequence estimate

$$\hat{\underline{I}} = \underline{I} + \underline{E} + \hat{\underline{E}} \quad .$$

The decoding algorithm is analogue to the classical Viterbi decoding scheme. Its complexity depends on the state space generated by the encoder G. It is not more complex then the Viterbi decoder, except for the circuitry to make the vector sequence $\underline{Z}\, H^{-1^T}$. Note that the Viterbi decoder compares the received data vector sequence $(\underline{I}\, G + \underline{N})$ with a possible transmitted codeword vector sequence $\hat{\underline{I}}\, G$, without using the matrix $[G^{-1}\ H^T]$.

In schematic form, for an additive white Gaussian noise channel (AWGN) with hard quantized matched filter outputs, the previously mentioned encoding and syndrome forming circuits, together with the inverse encoder G^{-1}, are used as indicated in Fig. 3. The task of the decoder is to make an estimate $\hat{\underline{E}}$ of $\underline{E}$, where $\underline{E} = \underline{N}\, G^{-1}$. The complexity of the above decoding schemes grows exponentially with the constraint length of the code. Long constraint length codes are therefore decoded with sequential decoding schemes. In the sequel, we will first explain the principles of a sequential decoding scheme, and then

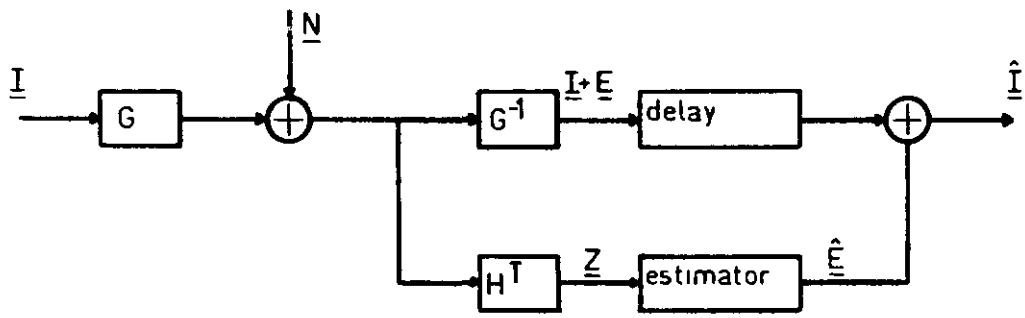

Fig. 3. Schematic use of a convolutional code.

describe the use of the information-correction decoder in sequential decoding.

In a Viterbi-like ML decoder, the complexity grows linearly with the number of states of the trellis diagram of the encoder G. For each state and each decoding step, the likelihood or metric, and the survivor must be calculated. As all survivor paths up to time t have the same lengths, the likelihood function in a hard decision decoder is proportional to the Hamming distance between the received sequence and a possible state sequence. Fano [7], introduced a metric that can be used in sequential decoding of tree codes, where paths could be of unequal length. For binary rate R=k/n tree codes, used on a BSC, the Fano-metric of a path $\underline{X}_i$ through the tree is

$$L_f(\underline{X}_i, \underline{Y}) = \sum_{j=0}^{N_i-1} \left(\log \frac{p(y_j \mid x_{ij})}{p(y_j)} - R\right) ,$$

where N_i is the length of $\underline{X}_i$, and y_j the received symbol at time instant j, $0 \leq j \leq N_i-1$. Note that $p(y_j \mid x_{ij})$ is equal to $p(n_j)$, where n_j is the channel noise if x_{ij} were transmitted. The "obvious" sequential decoding algorithm is the one which stores the Fano metric for all paths already been explored, and then

extends the path with the highest metric. As convolutional codes can be considered as a special class of tree codes, namely linear trellis codes, the above method can be used as a technique for the sequential decoding of convolutional codes.

We now give a short description of sequential stack decoding (SSD). The stack decoder stores in order of decreasing metric the explored paths in a stack. At each step the top path of the stack is extended. The extensions of a given path are regarded as new paths, and the old path is deleted from the stack. The decoder continues in the above way until the end of the trellis is reached. The case where the trellis has both a starting and an end point is referred to as frame decoding. The major problem with SSD is that of stack overflow. This occurs if the channel is noisy, and the stack size relatively small. Overflow means that the bottom path has been deleted. If the number of computations is so large that the end of the trellis can not be reached within a certain time interval, a frame erasure occurs. The particular information block must then be retransmitted, thus lowering the effective rate. One could also simply take the inverse to the received code sequence as an estimate for the information block, but then the error probability increases.

In contrast with SSD, for the Fano algorithm [8], progress in the decoding tree is made one node at the time, forward as well as backward. This leads to an algorithm with smaller memory requirements, but many more computations for a frame to be decoded.

As stated before, the SSD algorithm tries to find a "good" path or generator state sequence through a tree (trellis). Every step in the decoding algorithm, implemented according to (9), the top path $\underline{\hat{E}}\,|_0^\tau$ of the stack is extended. For rate k/n, 2^k successors are restored in the stack. As we restrict ourselves to minimal encoders G, only ν components of $\underline{\hat{E}}\,|_0^\tau$ suffice to compute

the metric values of the above successors. Fig. 4 gives a flowchart of the algorithm.

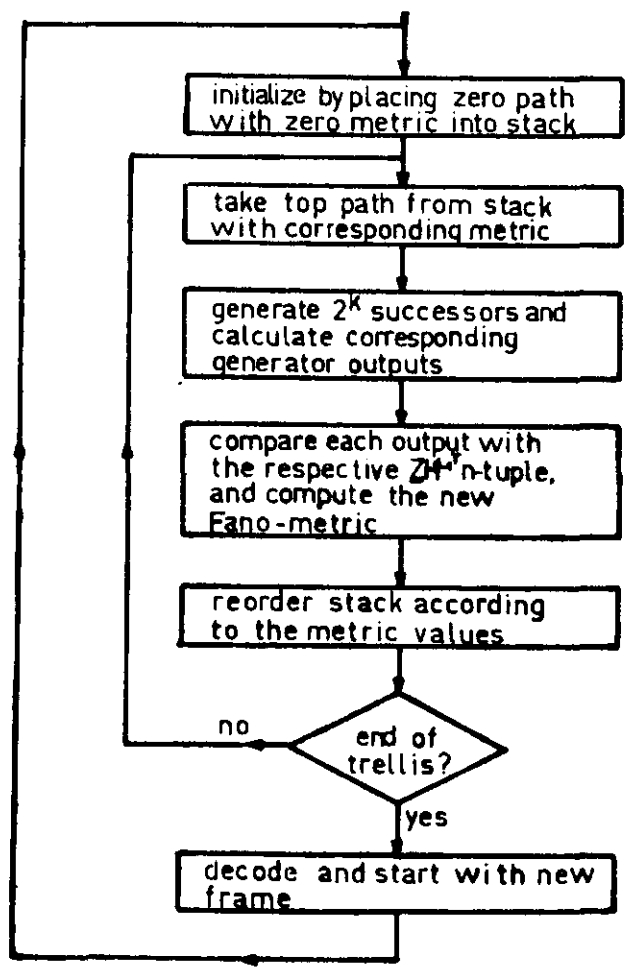

Fig. 4. SSD algorithm using the inverse to $[G^{-1} H^T]$.

Information-correction decoding according to (9) can be used in conjunction with either Fano- or stack decoding as described above. State space symmetries [1,2,3] of the syndrome former H^T can be used to reduce the complexity (hardware) of the ML-syndrome decoder. In the next section we use state space symmetries of the encoder G to obtain savings in sequential decoding.

Special rate k/n codes - savings in the number of computations

We first introduce the class $L_{n,\nu,\ell}$ of rate 1/n binary convolutional codes $(A,B,C,\ldots,D)$, i.e. in terms of their encoder connection polynomials. This class exhibits symmetries that allow for savings in the number of computations in sequential decoding. To wit $(A,B,C,\ldots,D) \in L_{n,\nu,\ell}$ iff

$$a_j = b_j \quad ; \quad 0 \leq j \leq \ell-1 \tag{10a}$$

$$C,\ldots,D \text{ all have delay} \geq \ell \tag{10b}$$

$$\gcd(A,B,C,\ldots,D) = 1 \tag{10c}$$

$$\max \deg.\ (A,B,C,\ldots,D) = \nu \quad . \tag{10d}$$

If condition (10c) is satisfied, then it follows from the invariant factor theorem [4], that the n-tuple $(A,B,C,\ldots,D)$ is a set of generator polynomials for some non-catastrophic rate 1/n convolutional code (in fact, for a class of such codes).

Each time unit extend a top path, $\hat{E}\,|_0^{\tau-1}$, of the stack to $\hat{E}\,|_0^{\tau}$ and compute

$$\underline{\hat{N}}\,|_0^{\tau} = (\hat{E}\,G + \underline{Z}\,H^{-1^T})\,|_0^{\tau} \quad , \tag{11}$$

in order to calculate the Fano metric of the path $\hat{E}\,|_0^{\tau}$. With each path in the stack we associate an index register $I[0:\ell-1]$. The content $C(I[i:i]) = 1$ if $(\hat{n}_1,\hat{n}_2,\hat{n}_3,\ldots,\hat{n}_n)^{\tau-i} = (0,1,\hat{n}_3,\ldots,\hat{n}_n)$, or $(1,0,\hat{n}_3,\ldots,\hat{n}_n)$, where $(\hat{n}_1,\hat{n}_2,\hat{n}_3,\ldots,\hat{n}_n)^{\tau-i}$ equals the noise vector at time $\tau-i$, otherwise $C(I[i:i]) = 0$. This index register plays an important role in the decoding algorithm, as will be shown in the following theorems.

Theorem 1: Let $(A,B,C,\ldots,D) \in L_{n,\nu,\ell}$. Then each path $\hat{E}\,|_0^{\tau-1}$ has a certain successor $\hat{E}\,|_0^{\tau}$. This successor has the property that there are $2^{\ell}-1$ other paths that have the same index register contents $C(I[\,0:\ell-1\,])$, and whose metric value follow easily from the metric value of the given successor.

Proof: Given the n-vector sequence $\underline{Z}\,H^{-1^T}\,|_0^{\tau}$ up to time τ, the content of stage $I[\,i:i\,]$ of the index register $I[\,0:\ell-1\,]$ of a path $\hat{E}\,|_0^{\tau}$ equals 1 if the corresponding, (11), sequence $\underline{\hat{N}}\,|_0^{\tau}$ has $(\hat{n}_1,\hat{n}_2)^{\tau-i} = (0,1)$, or $(1,0)$. Hence, knowing the successor $\hat{E}\,|_0^{\tau}$, together with its index register and metric value, we can construct $2^{|I|}-1$, where $|I|$ denotes the number of ones in the index-register, other paths with the same metric value. These paths only differ in a linear combination of $\{D^{\tau-i+1}\,E_c^{\,i}\,;\ 0\leq i\leq \ell-1\}$, where $E_c^{\,i} \triangleq (1,1,0,\ldots,0)\,G^{-1}\,|_0^{i-1}$. Now let us assume that whenever $(\hat{n}_1,\hat{n}_2)^{\tau} \neq (0,1)$, or $(1,0)$, we always extend a path with $(\hat{n}_1,\hat{n}_2)^{\tau}$ equal to $(0,0)$. As $a_0 = b_0 = 1$, we know that this is possible. Then, the zero's in the index register can be used to construct paths, also differing by a linear combination of $\{D^{\tau-i+1}\,E_c^{\,i}\ ,\ 0\leq i\leq \ell-1\}$, but with lower metric values. Whenever $(\hat{n}_1,\hat{n}_2)^{\tau-i}$ was equal to $(0,0)$, we know that there are other paths with $(\hat{n}_1,\hat{n}_2)^{\tau-i}$ equal to $(1,1)$. The metric values for these paths are easily calculated from the metric value of path $\hat{E}\,|_0^{\tau}$. Hence, instead of one path, we know 2^{ℓ} paths together with their metric values. Note that for $i=\ell$, and $(A,B,C,\ldots,D) \in L_{n,\nu,\ell}$, adding $D^{\tau-\ell+1}\,E_c^{\,\ell}$, influences the value of $(\hat{n}_1,\hat{n}_2,\ldots,\hat{n}_n)^{\tau}$. Q.E.D.

We will now show that extending the representative member $\hat{E}\,|_0^{\tau}$ (i.e. the member with highest metric) of a class of 2^{ℓ} paths suffices to extend each member of this class.

Theorem 2: Let $(A,B,C,\ldots,D) \in L_{n,\nu,\ell}$ and $\hat{E}\,|_0^{\tau-1}$ a path according to Theorem 1, then the 2^{ℓ} paths represented by $\hat{E}\,|_0^{\tau-1}$, can be extended simultaneously:

Proof: Extend the representative path $\hat{E}\,|_0^{\tau-1}$ such that $\underline{\hat{N}}\,|_\tau^\tau$ according to (11) has $(\hat{n}_1,\hat{n}_2)^\tau \neq (1,1)$. The successor $\hat{E}\,|_0^\tau$ then represents a new class of 2^ℓ paths. The index register of the original path $\hat{E}\,|_0^{\tau-1}$ is updated as follows. Right shift $I\left[0:\ell-1\right]$ by one place, dropping $C(I\left[\ell-1:\ell-1\right])$ and set $I\left[0:0\right]$ according to $C(I\left[0:0\right]) \leftarrow (\hat{n}_1 \oplus \hat{n}_2)^\tau$. However, as (C,...,D) all have delay $\geq \ell$, and $a_\ell \neq b_\ell$ or $c_\ell,\ldots,d_\ell \neq 0$, the paths differing by $D^{\tau-\ell}\,E_c^{\ell-1}$ from $\hat{E}\,|_0^{\tau-1}$ give a change in $(\hat{n}_1,\hat{n}_2,\hat{n}_3,\ldots,\hat{n}_n)^\tau$. When $C(I\left[\ell-1:\ell-1\right]) = 1$, we simply add $D^{\tau-\ell}\,E_c^{\ell-1}$ to $\hat{E}\,|_0^{\tau-1}$, and calculate a successor according to Theorem 1. The updated index register contents of this successor $\hat{E}'\,|_0^\tau$ can be obtained as described above. A value $C(I\left[\ell-1:\ell-1\right]) = 0$ indicates $(\hat{n}_1,\hat{n}_2)^{\tau-\ell} = (0,0)$, or (1,1). In this case the second extension, i.e. from $\hat{E}\,|_0^{\tau-1}$ to $\hat{E}'\,|_0^\tau$, requires an adjustment of the metric value. As the successor $\hat{E}\,|_0^\tau$ has $(\hat{n}_1,\hat{n}_2)^{\tau-\ell} = (0,0)$ and $\hat{E}'\,|_0^\tau$ has $(\hat{n}'_1,\hat{n}'_2)^{\tau-\ell} = (1,1)$, the metric value of $\hat{E}'\,|_0^\tau$ has to be decreased by the metric contribution of $(\hat{n}'_1,\hat{n}'_2)^{\tau-\ell} = (1,1)$. Hence, we have extended the 2^ℓ paths represented by $\hat{E}\,|_0^{\tau-1}$, using only this one path, its index register, and its metric value. Q.E.D.

We now extend our results, i.e. the class $L_{n,\nu,\ell}$, for rate 1/n codes to apply for general rate k/n codes.

Let G represent a rate k/n minimal convolutional encoder, with the first row $\in L_{n,\nu_1,\ell}$, and overall constraint length ν. According to the definition of a minimal encoder, there are no other rows, or linear combinations, that are $\in L_{n,\nu_j,\ell'}$, $1<j\leq k$, $1\leq\ell'$. For suppose there exists such a linear combination, then we can always reduce the overall constraint length of the code. Theorem 1, and 2 can now be used on the class of rate k/n codes. The first component $\hat{E}_1\,|_0^{\tau-1}$ of the vector sequence $\underline{\hat{E}}\,|_0^{\tau-1}$ now enables us to again define the sets of 2^ℓ paths.

To illustrate the decoding algorithm, we take an example from [8, chapter 6, p. 7], where a received data sequence of a rate $\frac{1}{2}$ code contains two

errors. The contribution to the Fano-metric of the noise pairs (0,0) , (0,1) , (1,0) , (1,1) equals +2 , -9 , -9 , -20, respectively. A developped path is followed by the corresponding Fano-metric in the L.H. part of Fig. 5, and by the content of the index register between parenthesis, and the value of the of the Fano-metric on the R.H. side of the same Figure. The decoding algorithms run until the correct path appears on the top of the stack. Observe a large difference in the number of computations, and in the storage requirements in favor of our algorithm !

Information : 1 0 1 0 0

Transmitted : 11 10 00 10 11

Received : $\underline{0}1$ 10 $0\underline{1}$ 10 11

Encoder : $G = (1+D+D^2 , 1+D^2)$

$Z H^{-1^T}$: 10 11 00 10 01

$\underline{N} G^{-1}$: 0 1 1 1 0

Basic stack algorithm		Modified stack algorithm	
time:	Stack content after reordening	time:	Stack content after reordening
1	0,-9 ; 1,-9	1	1(1),-9
2	1,-9 ; 00,-18 ; 01,-18	2	01(0),-7 ; 10(1),-18
3	10,-7 ; 00,-18 ; 01,-18 ; 11,-29	3	011(1),-16 ; 10(1),-18 ; 000(0),-27
4	100,-16 ; 101,-16 ; 00,-18 ; 01,-18 ; 11,-29	4	0111(0),-14 ; 101(1),-18 ; 0100(1),-25 ; 000(0),-27
5	101,-16 ; 00,-18 ; 01,-18 ; 1000,-25 ; 1001,-25 ; 11,-29	5	01110(0),-12 ; 101(1),-18 ; 0100(1),-25 ; 000(0),-27 ; 01101(1),-45
6	1010,-14 ; 00,-18 ; 01,-18 ; 1000,-25 ; 1001,-25 ; 11,-29 ; 1011,-36		
7	10100,-12 ; 00,-18 ; 01,-18 ; 1000,-25 ; 1001,-25 ; 11,-29 ; 10101,-34 ; 1011,-36		

Fig. 5. Decoding example for the basic as well as for the modified stack algorithm.

Quantization of the received data symbols

As pointed out in [8], binary phase shift keying (BPSK) in combination with coding is an efficient way of communication over the AWGN channel. Quantization of the demodulated received data symbols, facilitates digital processing at the decoder. When 8-level quantization is used, about 0.25dB in received signal to noise ratio is lost as compared with infinitely fine quantization. With 2-level (binary) quantization the loss in SNR is roughly 2 dB. Fig. 6 shows the quantization scheme for 4 levels, where +1 corresponds with a data symbol 1, and -1 with a

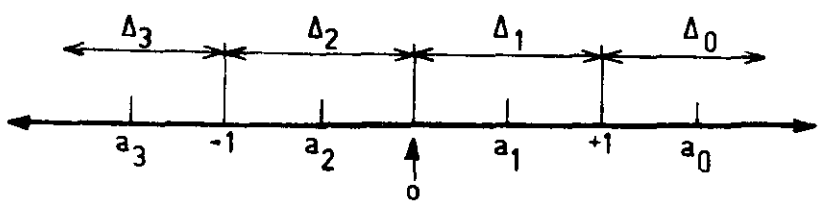

Fig. 6. Quantization scheme for 4 levels

data symbol 0. The spacings in the above scheme can be shown to be almost optimum. The Gaussian channel with modulator and demodulator is then equivalent to a discrete channel with two inputs and 4 outputs. The channel transition probabilities are equal to the probabilities that a Gaussian random variable with variance $\sqrt{\frac{N_0}{2E}}$ and mean ± 1 lies in the intervals indicated in Fig. 6. The problem we are now faced with is the adjustment of the message-correction decoder. Take, for example, the transition probability diagram for a converted channel with 2 inputs and 4 outputs as indicated in Fig. 7. Let a received signal lie in interval Δ_2. The syndrome forming circuit only accepts the symbols 0 and 1. Hence, a binary quantizer is used to set the received signal equal to 0. Now there are two possibilities, the relevant noise digit could either be zero or one with probability $Pr(0) = q_1$ and

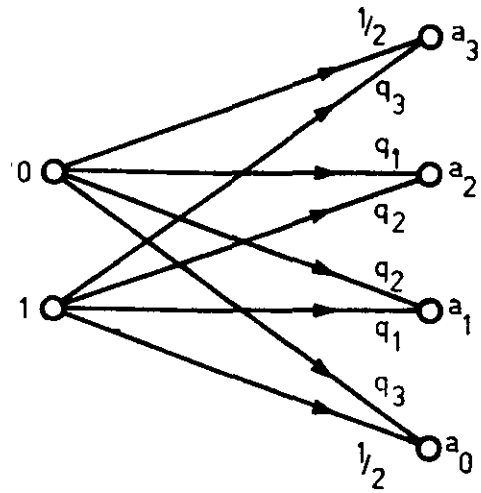

Fig. 7. Transition probability diagram for 4-level quantization.

$Pr(1) = q_2$, respectively. The same can be said about a received signal lying in interval 1. For the intervals 0 and 3 , $Pr(0) = \frac{1}{2}$ and $Pr(1) = q_3$. In fact, we only need the absolute value of the received signal to determine Pr(0) and Pr(1). For each extension made in the sequential decoder, we are now able to calculate the corresponding Fano-metric.

In order to obtain reduction in our sequential decoder, we used the fact that in a two-level quantized AWGN channel, the contribution of a noise pair $(\hat{n}_2,\hat{n}_1) = (0,1)$ to a path metric equals that of the complementary pair. It is easy to see, that with the above quantization schemes, this is no longer true. However, if we extend a class of paths, we may store the representative with highest Fano-metric. The index register now indicates that there is another possible extension , in the same sence as described in the previous section, but with lower metric. This means that the essence of the algorithm remains unchanged. Unlikely paths are again extended together with the more likely one(s). Fig. 8 gives a possible contribution scheme for calculating the Fano-metric contribution of the relevant noise pairs, in the case of a rate $\frac{1}{2}$ code and SNR of 4 dB.

intervals of received data pair	contribution for the noise pairs			
	00	01	10	11
Δ_0 , Δ_0	1	-8.5	-8.5	-18
Δ_0 , Δ_1	0.8	-2.5	-8.7	-12
Δ_0 , Δ_2	0.8	-2.5	-8.7	-12
Δ_0 , Δ_3	1	-8.5	-8.5	-18
Δ_1 , Δ_0	0.8	-8.7	-2.5	-12
Δ_1 , Δ_1	0.6	-2.7	-2.7	- 6
Δ_1 , Δ_2	0.6	-2.7	-2.7	- 6
Δ_1 , Δ_3	0.8	-8.7	-2.5	-12
Δ_2 , Δ_0	0.8	-8.7	-2.5	-12
Δ_2 , Δ_1	0.6	-2.7	-2.7	- 6
Δ_2 , Δ_2	0.6	-2.7	-2.7	- 6
Δ_2 , Δ_3	0.8	-8.7	-2.5	-12
Δ_3 , Δ_0	1	-8.5	-8.5	-18
Δ_3 , Δ_1	0.8	-2.5	-8.7	-12
Δ_3 , Δ_2	0.8	-2.5	-8.7	-12
Δ_3 , Δ_3	1	-8.5	-8.5	-18

Fig. 8. Contributions to the Fano-metric of noise pairs (0,0) , (0,1) , (1,0) and (1,1) , in the case of 4-level quantization and SNR of 4 dB.

Note that an extension according to Theorems 1 and 2 is very easy. We stored the best successor, and as can be seen from Fig. 8, the complementary transition has a contribution to the Fano-metric that is easy to calculate from the stored one.

Hence, knowing the respective intervals, and the index register contents, the metric of a path less likely then the stored one can be found from a table, like given in Fig. 8.

Column Distance Function

The column distance function (CDF) of a convolutional code is defined as

$$d_c(r) = \min_{d_1^{ij} \neq 0} \sum_{s=1}^{r} d_s^{ij} ,$$

where d_s^{ij} denotes the Hamming distance between the s branches of two codewords $\underline{x}^i$ and $\underline{x}^j$, respectively. Johannesson [9] intruduced the distance profile of a rate 1/n convolutional code as the $(\nu+1)$-tuple $\underline{d} = (d_c(1), d_c(2), \ldots, d_c(\nu+1))$, where ν is referred to as the constraint length of the code. He defined a distance profile $\underline{d}$ to be superior to $\underline{d}'$ if $d_c(j) > d_c'(j)$, for the smallest index j, $1 \leq j \leq \nu+1$, where $d_c(j) \neq d_c'(j)$. It has been shown [10], that rapid column distance growth minimizes the decoding effort, and therefore the probability of decoding failure. An ODP ensures that for the first constraint length, the column distance grows as rapidly as possible. However, the class of codes with an ODP, is quite different from the class $L_{n,\nu,\ell}$ of codes that leads to savings in decoder complexity, $L_{2,\nu,1}$, being the only exception. Table 1 gives the distance profile for the class $L_{2,2\ell,\ell}$, for various values of ℓ. It is obvious that $d_c(\ell) = 2$, and hence, the distance profile gets worse for increasing ℓ. Table 2 lists the distance profile for some classes $L_{2,\nu,\ell}$, $4 \leq \nu \leq 22$, and some values of ℓ, $1 \leq \ell \leq 10$. The searches were not exhaustive.

Figs. 9 and 10, illustrate the movement of the modified sequential stack decoder in order to decode the noise pairs (0,1), and (1,1), respectively. The initial components of the distance profile are equal to $2,2,2,3,4,5,\ldots,\ell = 3$ and the contributions of the noise pairs (0,0) , (0,1) , (1,0) , (1,1) to the Fano-metric are +1 , -4 , -4 , -9 , respectively. The same is done for an ODP-code, using the standard stack decoder, and initial distance profile components $2,3,3,4,4,5,\ldots$. These results are illustrated in Figs. 11 and 12. Indicated

ν	ℓ	distance profile
4	1	2 3 3 4 4
6	2	2 2 3 4 4 4 5
6	1	2 3 3 4 4 5 5
8	3	2 2 2 3 4 5 5 5 5
8	2	2 2 3 4 4 4 5 5 6
8	1	2 3 3 4 4 5 5 6 6
10	4	2 2 2 2 3 4 5 5 5 6 6
10	3	2 2 2 3 4 5 5 5 5 6 6
10	2	2 2 3 4 4 4 5 5 6 6 6
10	1	2 3 3 4 4 5 5 6 6 6 7
12	5	2 2 2 2 2 3 4 5 5 6 6 6 6
14	6	2 2 2 2 2 2 3 4 5 5 6 7 7 7 7
14	1	2 3 3 4 4 5 5 6 6 6 7 7 8 8 8
16	7	2 2 2 2 2 2 2 3 4 5 5 6 7 7 7 8 8
18	8	2 2 2 2 2 2 2 2 3 4 5 5 6 7 7 8 8 8 8
20	9	2 2 2 2 2 2 2 2 2 3 4 5 5 6 7 7 8 8 8 8 8
22	10	2 2 2 2 2 2 2 2 2 2 3 4 5 5 6 7 7 8 8 9 9 9 9

Table 1. Listing of distance profile in the class $L_{2,2\ell,\ell}$ $1 \leq \ell \leq 15$.

ℓ	distance profile
1	2 3 3
2	2 2 3 4 4
3	2 2 2 3 4 5 5
4	2 2 2 2 3 4 5 5 5
5	2 2 2 2 2 3 4 5 5 6 6
6	2 2 2 2 2 2 3 4 5 5 6 7 7
7	2 2 2 2 2 2 2 3 4 5 5 6 7 7 7
8	2 2 2 2 2 2 2 2 3 4 5 5 6 7 7 8 8
9	2 2 2 2 2 2 2 2 2 3 4 5 5 6 7 7 8 8 8
10	2 2 2 2 2 2 2 2 2 2 3 4 5 5 6 7 7 8 8 9 9
11	2 2 2 2 2 2 2 2 2 2 2 3 4 5 5 6 7 7 8 8 9 9 9
12	2 2 2 2 2 2 2 2 2 2 2 2 3 4 5 5 6 7 7 8 8 9 9 10 10
13	2 2 2 2 2 2 2 2 2 2 2 2 2 3 4 5 5 6 7 7 8 8 9 9 10 10 10
14	2 2 2 2 2 2 2 2 2 2 2 2 2 2 3 4 5 5 6 7 7 8 8 9 9 10 10 11 11
15	2 2 2 2 2 2 2 2 2 2 2 2 2 2 2 3 4 5 5 6 7 7 8 8 9 9 10 10 11 11 11

Table 2. Listing of distance profile for some classes $4 \leq \nu \leq 22$, $1 \leq \ell \leq 10$.

along the vertical axis is the Fano-metric. Each arrow indicates a path that has been stored in the stack.

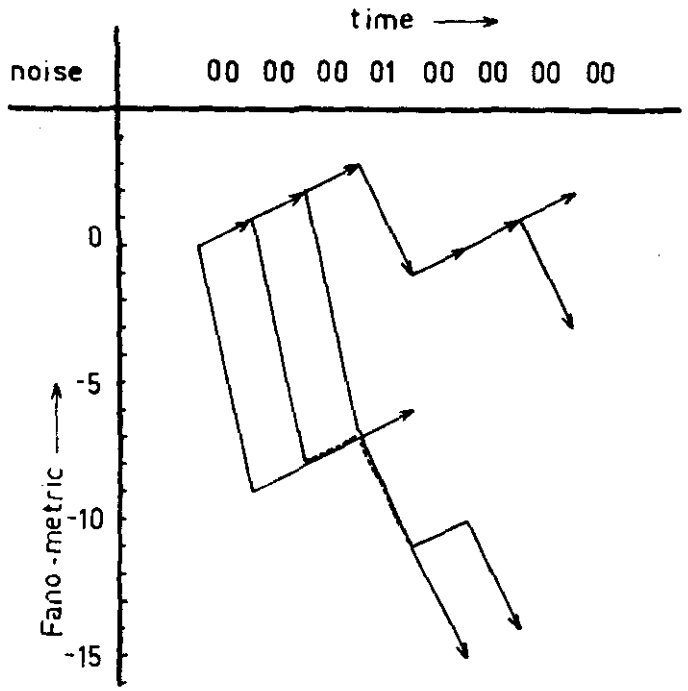

Fig. 9. Movements of a modified sequential stack decoder in order to decode a noise pair (0,1).

Note the absence of multiple arrows in Fig. 9. In Fig. 10 only two extra extensions have been made. Comparing these figures with Figs. 11, and 12, for ODP codes with standard decoding, respectively, one observes many additional decoder extensions for the same noise patterns.

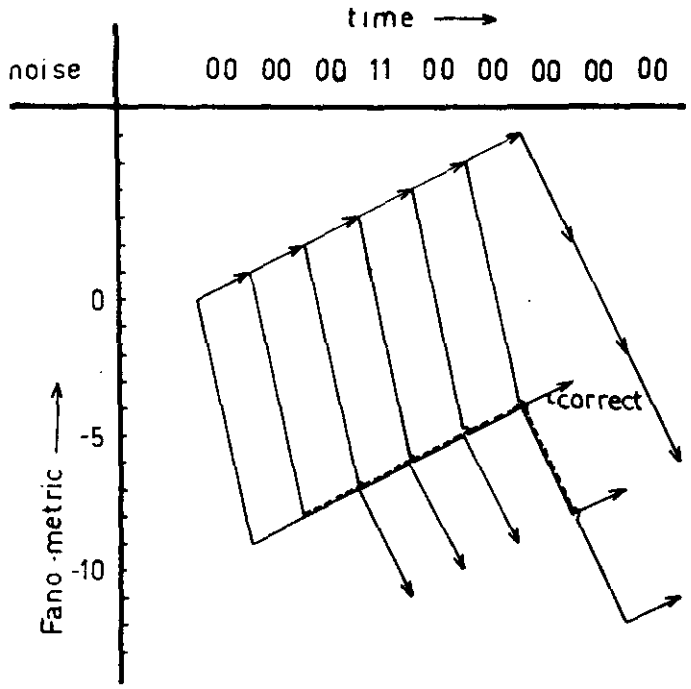

Fig. 10. Movements of a modified sequential stack decoder in order to decode a noise pair (1,1).

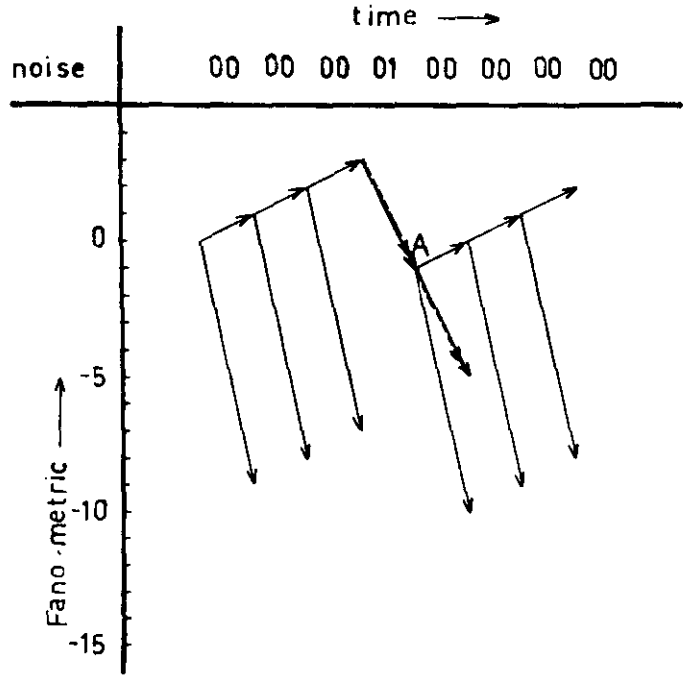

Fig. 11. Movements of a standard stack decoder to decode a noise pair (0,1).

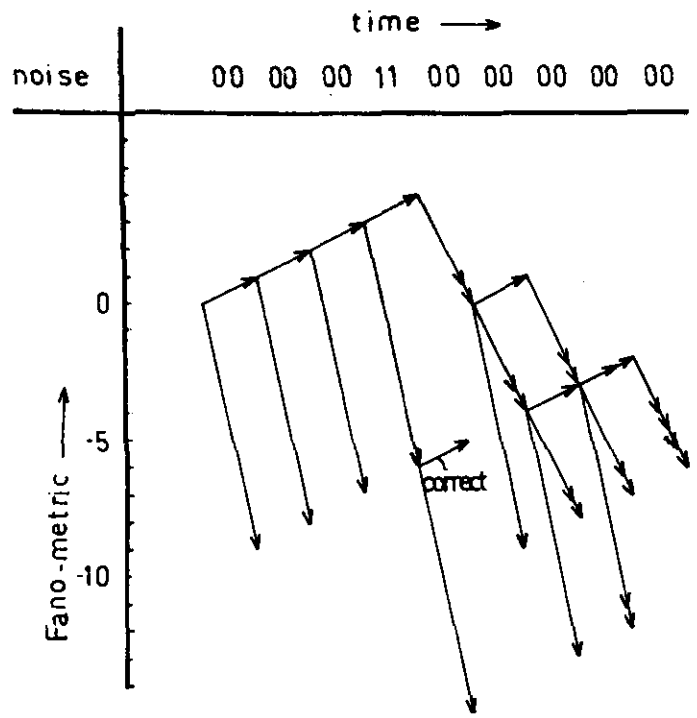

Fig. 12. Movements of a standard stack decoder to decode a noise pair (1,1).

Measurements

Information-correction decoding has been applied to SSD. The encoded information is transmitted over a BSC. A particular simulation run consists of 10,000 decoded frames of 256 information digits followed by ν tail digits each. The maximum size of the decoder stack was set equal to 1000. The simulation results are summarized in the Figures. We plot the distribution of the normalized number of computations, N/L, per frame, where $L = 256 + \nu$ is the frame length.

The ODP [9,10] is an important parameter in sequential decoding. Hence, our initial simulation runs apply to ODP codes. The results are given in Figs. 12, and 13. Observe that the distribution of the number of computations does not change appreciable if we increase ν beyond the value $\nu = 10$. The dependance of the results in Figs. 12, and 13 on ν for small values of $\nu < 10$ is a result of

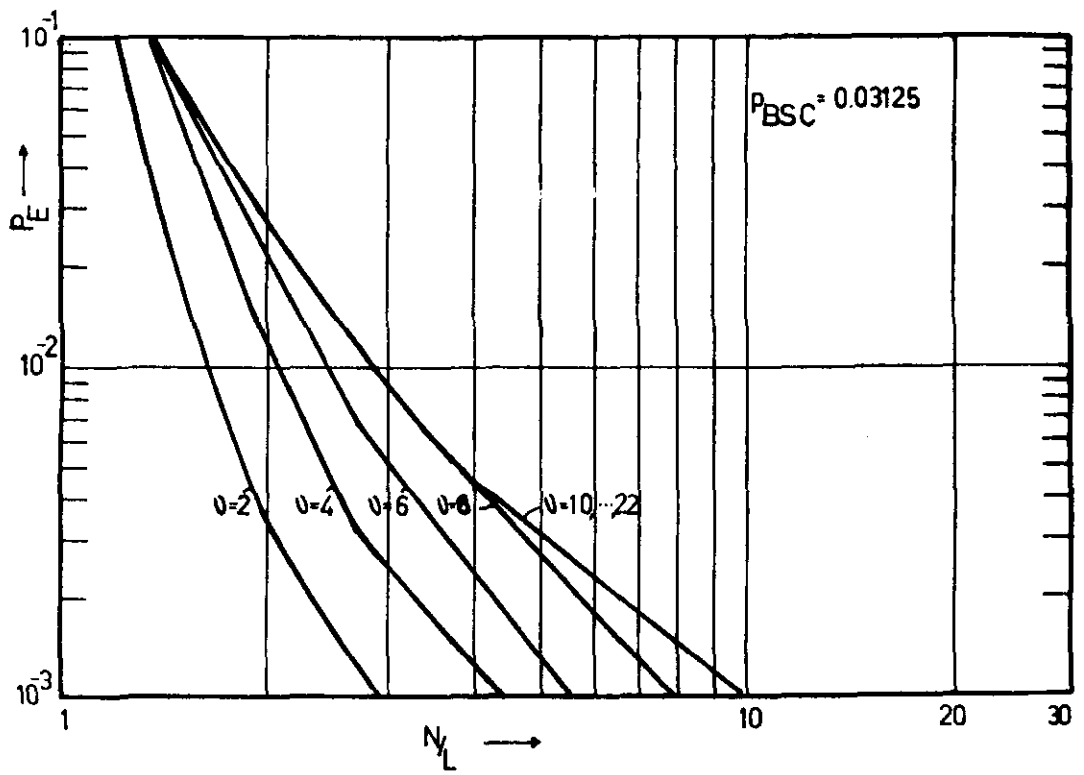

Fig. 12. Distribution of the number of computations per frame for ODP codes with classical stack decoding and $P_{BSC} = 0.03125$.

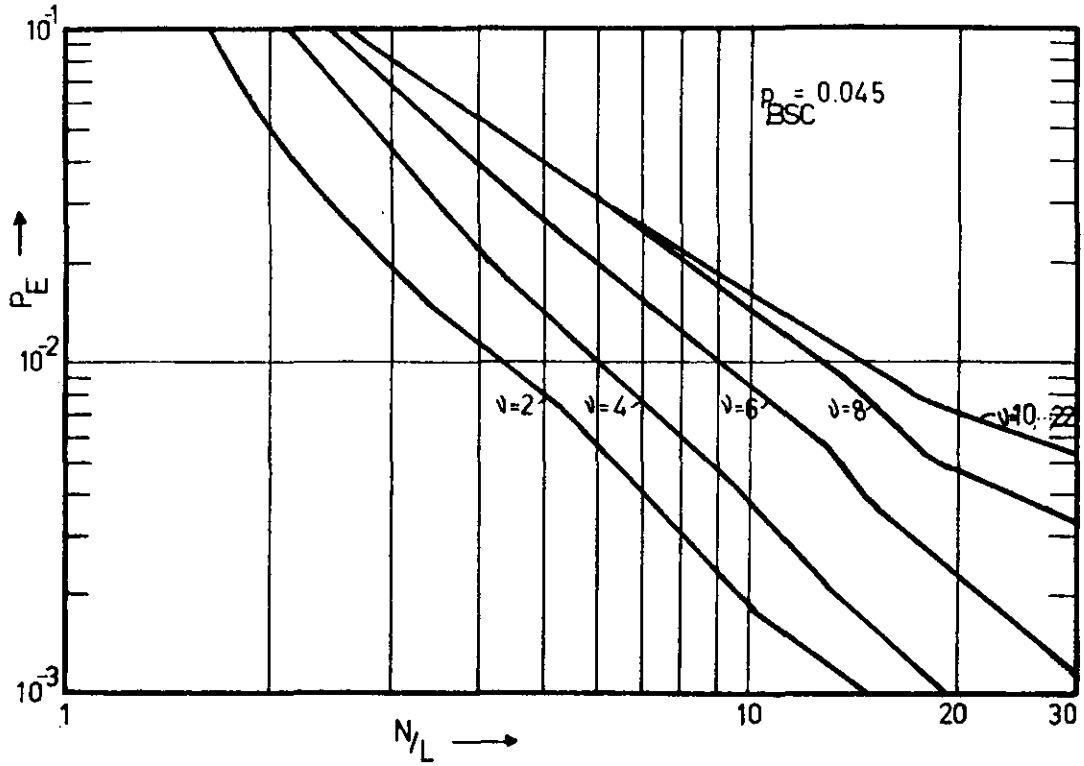

Fig. 13. Distribution of the number of computations per frame for ODP codes with classical stack decoding and $P_{BSC} = 0.045$.

the trellis structure of convolutional codes. If we neglect the effect of frame erasures, the advantage that accrues from using long constraint length codes is an improvement in the undetected error rate. The $\nu = 10$ ODP code, is taken as a reference code in later simulation runs. This code has a free distance,[5], of 14.

Fig. 14 illustrates the performance of codes in the class $L_{2,\nu,\ell}$, using classical stack decoding. Note the influence of the distance profile for large values of ℓ.

Figs. 15, and 16 apply to Fano or stack decoders, that make use of the "metric equivalence" as defined in [1,2,3] . In stack decoding a further

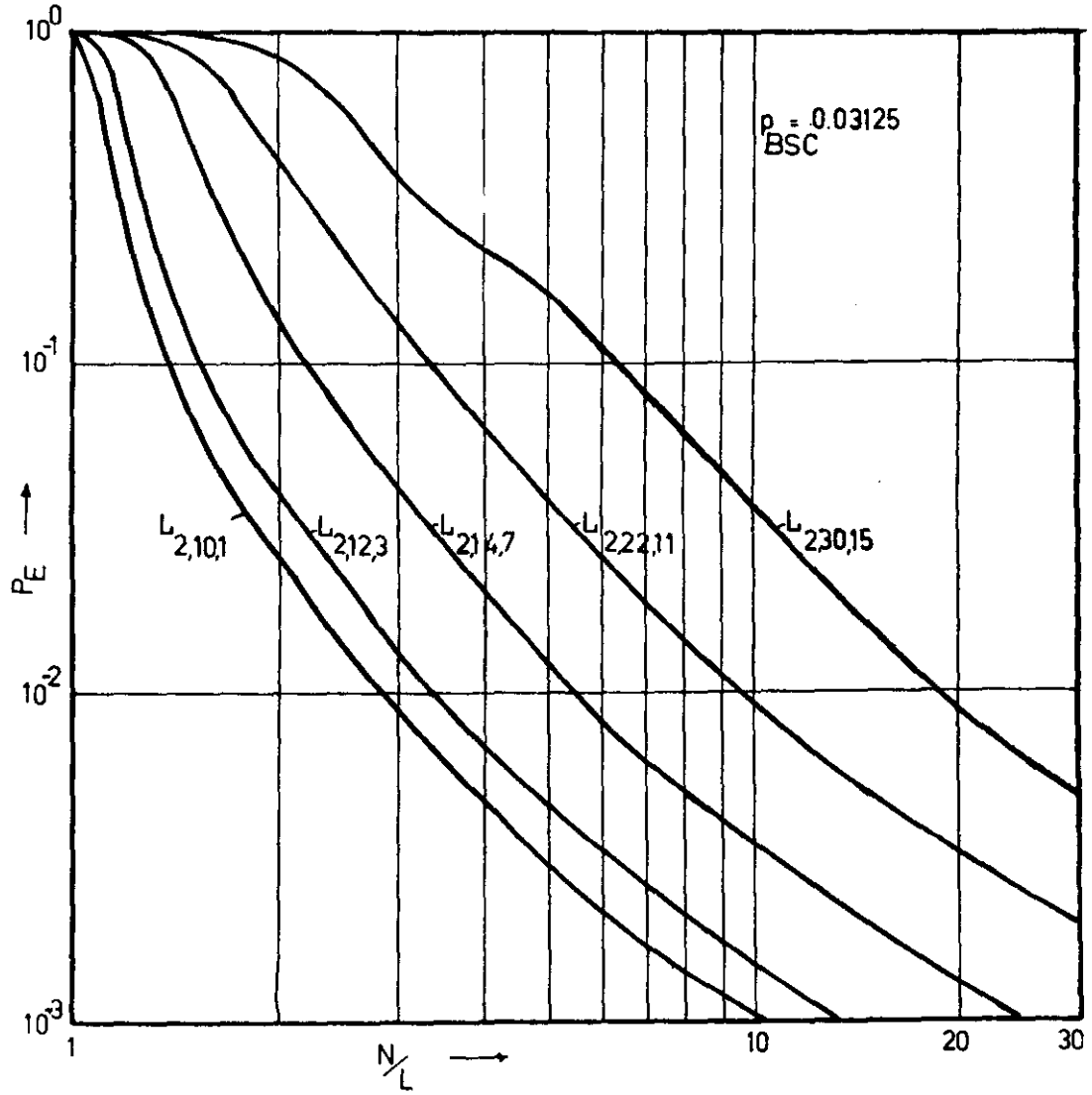

Fig. 14. Distribution of the number of computations per frame for $L_{2,\nu,\ell}$, with classical stack decoding.

reduction in the number of computations can be obtained by using the results described by Theorems 1, and 2. These latter results for the information-correction decoder are given in Figs. 17, and 18. Note that these results are better than those obtained with ODP codes, and classical stack decoding.

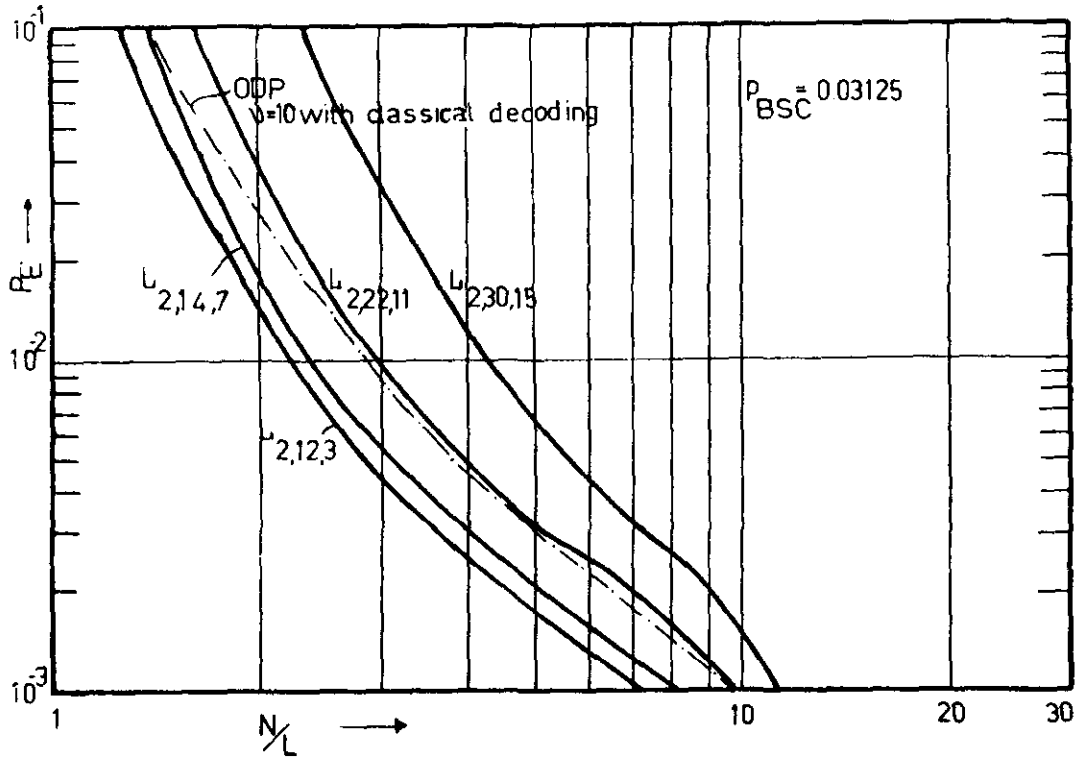

Fig. 15. Distribution of the number of computations per frame with a stack decoder that uses "metric equivalence", and $P_{BSC} = 0.03125$.

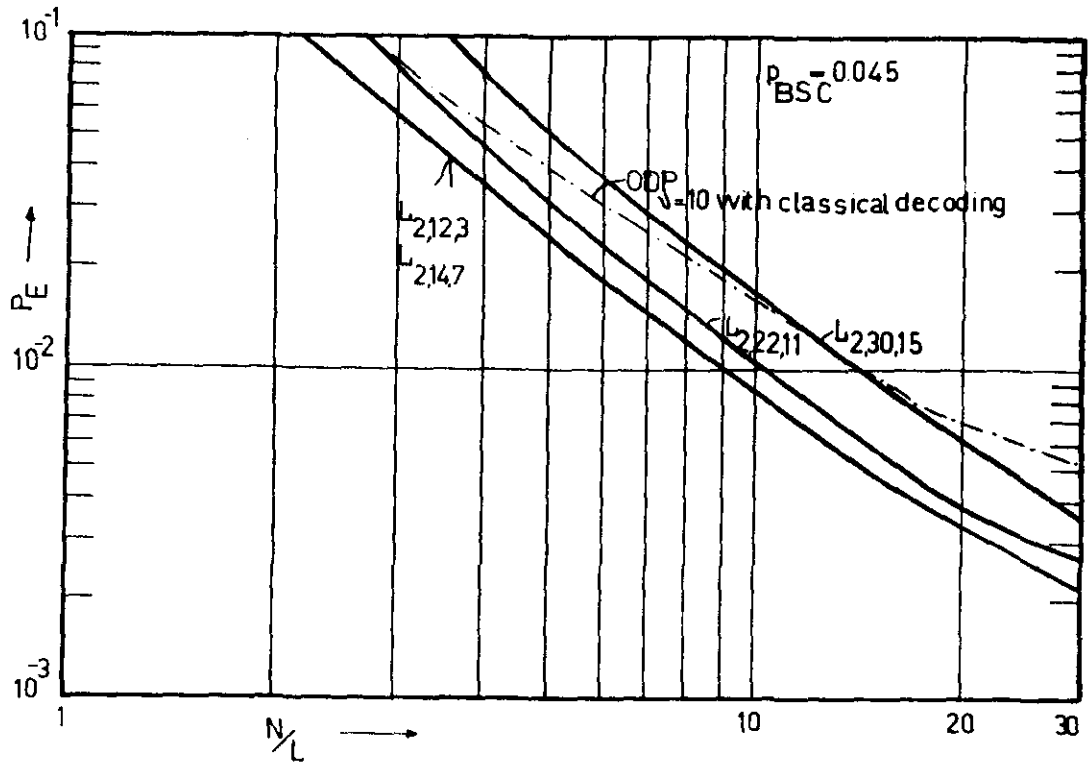

Fig. 16. Distribution of the number of computations per frame with a stack decoder that uses "metric equivalence", and $P_{BSC} = 0.045$.

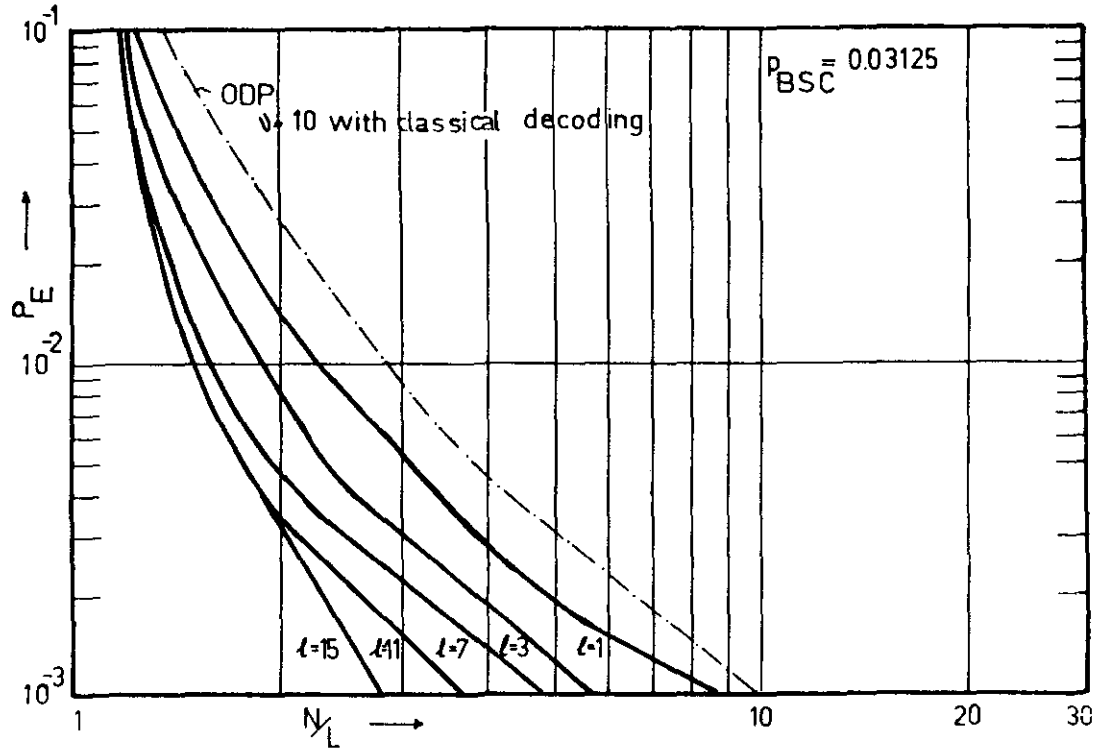

Fig. 17. Distribution of the number of computations per frame for codes in $L_{2,\nu,\ell}$ and decoding according to Theorems 1, and 2, and $P_{BSC} = 0.03125$.

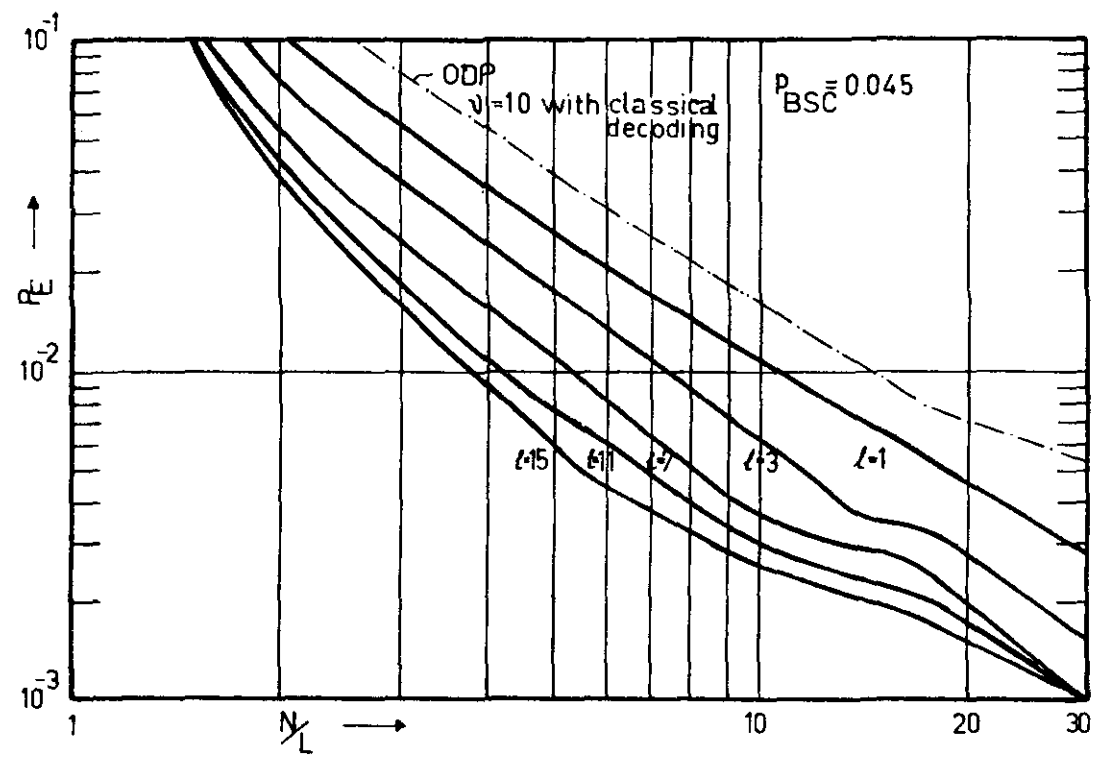

Fig. 18. Distribution of the number of computations per frame for codes in $L_{2,\nu,\ell}$ and decoding according to Theorems 1, and 2, and $P_{BSC} = 0.045$

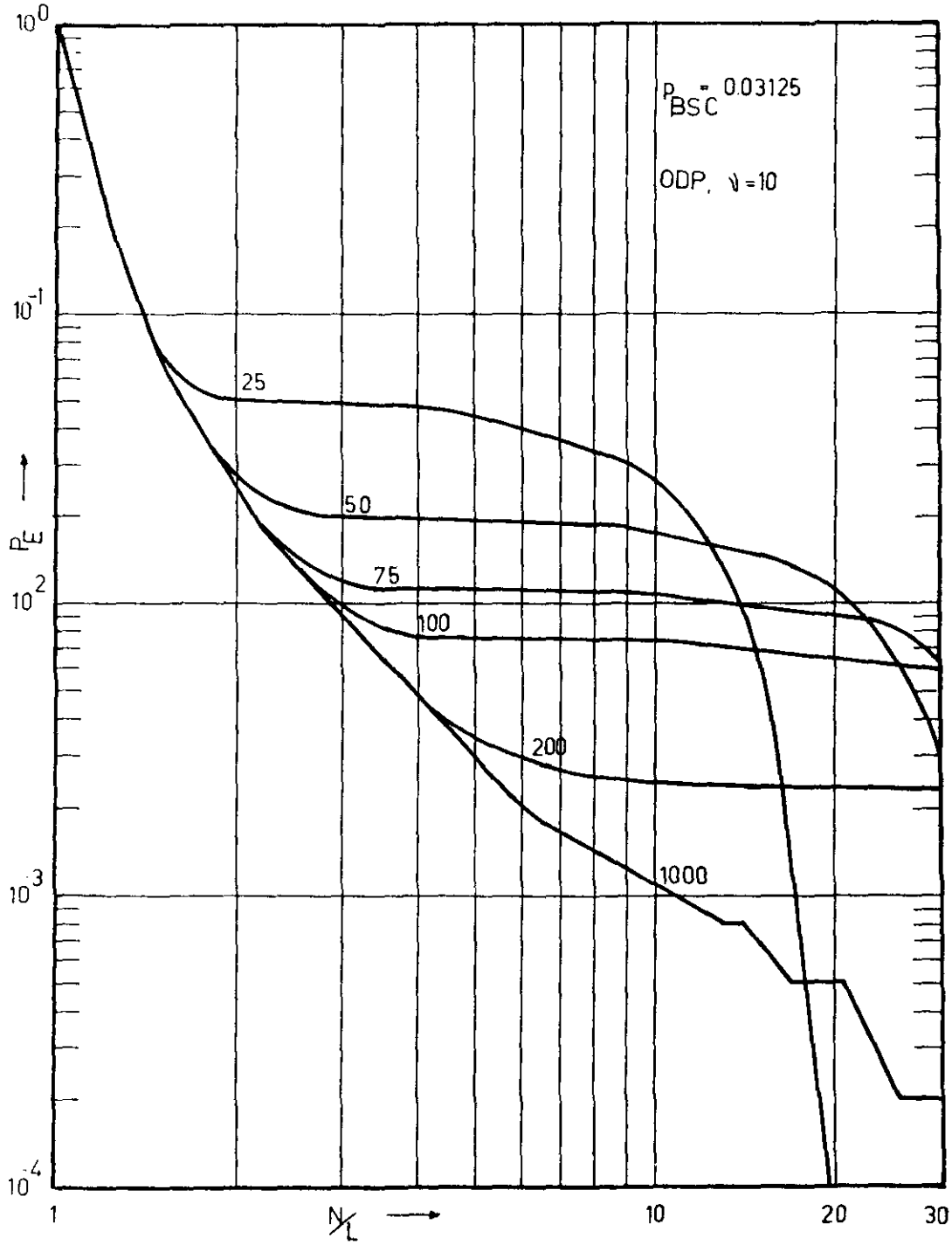

Fig. 19. Distribution of the number of computations per frame for the ODP $\nu = 10$ code with classical stack decoding at various values of the stack depth.

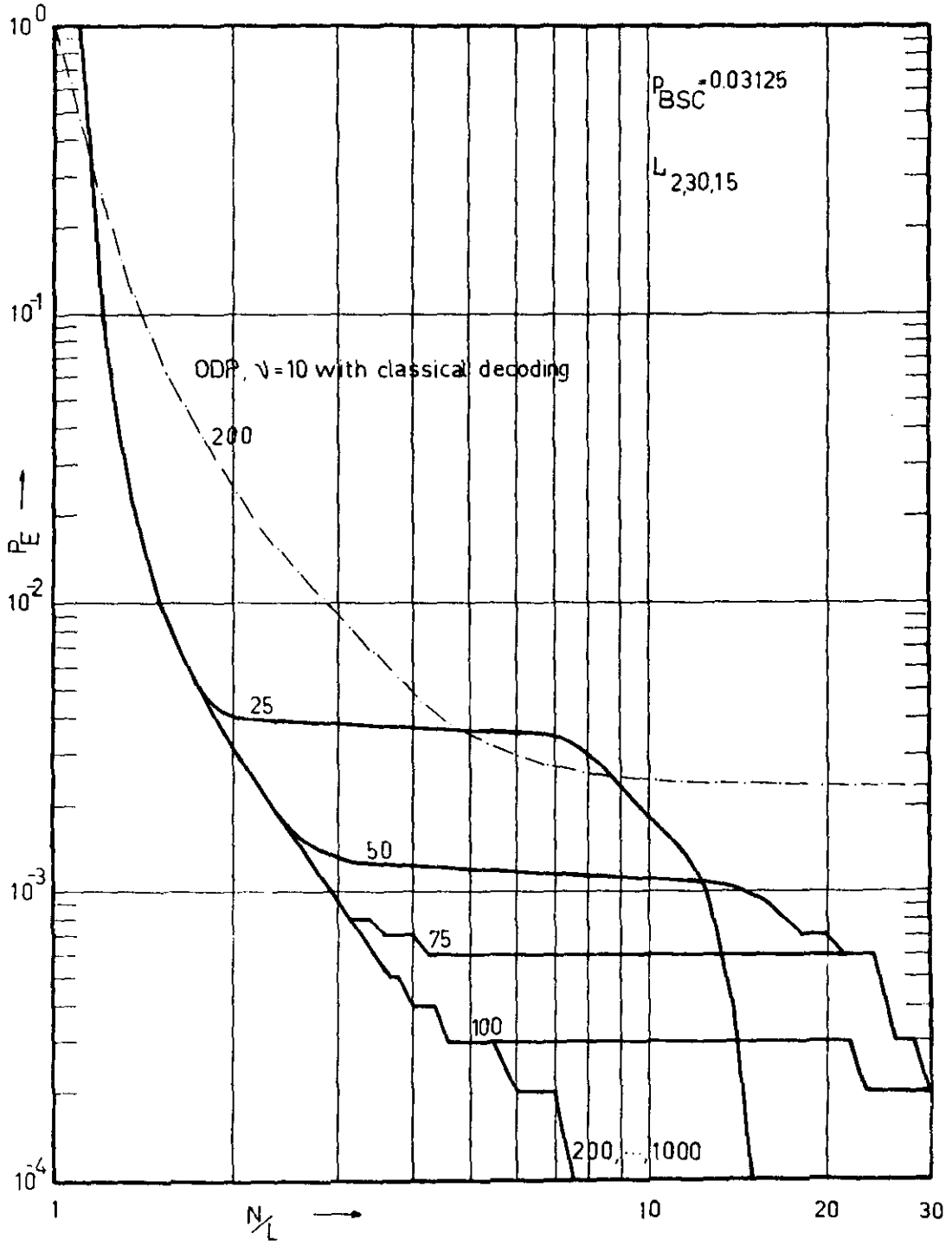

Fig. 20. Distribution of the number of computations per frame for the code in $L_{2,30,15}$, with decoding according to Theorems 1, and 2, at various values of the stack depth.

stack depth	number of frames in error		number of frames with $N_L > 30$	
	classical	modified	classical	modified
25	515	39	0	0
50	170	13	30	2
75	49	7	64	3
100	20	5	57	2
200	3	5	23	1
500	4	5	5	1
1000	3	5	2	0

Fig. 21. Comparison in the number of frames in error and the number of erased frames for the codes of Figs. 19, and 20, respectively.

Conclusions

It has been shown, that the inverse polynomial matrix $\begin{bmatrix} G \\ H^{-1^T} \end{bmatrix}$ to $[\, G^{-1} \; H^T \,]$ can be used to decode convolutional codes. We refer to this method of decoding as information-correction decoding. The complexity of this decoding procudure is comparable to that of the classical Viterbi decoder. However, in sequential decoding a reduction in the erasure probability can be obtained by using symmetries of the encoder G.

As far as ML decoding is concerned, the information-correction decoding algorithm could lead to a reduced state decoder. For, the vector sequences $\underline{Z}\, H^{-1^T}$ and $\hat{\underline{E}}\, G$ together define a noise estimate $\hat{\underline{N}}$, unlikely paths can be discarded from the trellis.

The free distance of our class $L_{n,\nu,\ell}$ of codes is less than that of the general class of convolutional codes. Prelimary results, however, indicate that the loss in free distance is of small importance, and good long codes can be found. The search for these codes can be simplified by using the very symmetries of $L_{n,\nu,\ell}$.

Acknowledgement

The authors want to thank their advisor Prof.dr.ir. J.P.M. Schalkwijk, and the students W.J.H.M. Lippmann and A.P.C. van Schendel for the contributions to this report, and Mrs. G. Driever-van Hulsen for the accurate typing of it.

References

[1] J.P.M. Schalkwijk and A.J. Vinck, "Syndrome decoding of convolutional codes", IEEE Trans. Commun. (Corresp.), vol. COM-23, pp. 789-792, July 1975.

[2] J.P.M. Schalkwijk and A.J. Vinck, "Syndrome decoding of binary rate $\frac{1}{2}$ convolutional codes", IEEE Trans. Commun., vol. COM-24, pp. 977-985, September 1976.

[3] J.P.M. Schalkwijk, A.J. Vinck and K.A. Post, "Syndrome decoding of binary rate k/n convolutional codes", IEEE Trans. Inform. Theory, vol. IT-24, pp. - , September 1978.

[4] G.D. Forney, Jr., "Convolutional codes I : Algebraic structure", IEEE Trans. Inform. Theory, vol. IT-16, pp. 720-738, November 1970; also, correction appears in vol. IT-17, p. 360, May 1971.

[5] A.J. Viterbi, "Convolutional codes and their performance in communication systems", IEEE Trans. Commun. (Special Issue on Error Correction Codes - Part II), vol. COM-19, pp. 751-772, October 1971.

[6] G.D. Forney, Jr., "Structural analysis of convolutional codes via dual codes", IEEE Trans. Inform. Theory, vol. IT-19, pp. 512-518, July 1973.

[7] R.M. Fano, "A heuristic discussion of probabilitic decoding", IEEE Trans. Inform. Theory, vol. IT-9, pp. 64-73, April 1973.

[8] A.J. Viterbi and J.K Omura, "Principles of Digital Communication and Coding", to appear.

[9] R. Johannesson, "Robustly-optimal rate one-half binary convolutional codes", IEEE Trans. Inform. Theory, vol. IT-21, pp. 464-468, July 1975.

[10] P.R. Chevillat and D.J. Costello, Jr., "A Non-Random Coding Analysis of Sequential Decoding", IEEE Trans. Inform. Theory, vol. IT-24, pp. 443-451, July 1978.

EINDHOVEN UNIVERSITY OF TECHNOLOGY
THE NETHERLANDS
DEPARTMENT OF ELECTRICAL ENGINEERING

Reports:

1) **Dijk, J., M. Jeuken and E.J. Maanders**
AN ANTENNA FOR A SATELLITE COMMUNICATION GROUND STATION (PROVISIONAL ELECTRICAL DESIGN).
TH-Report 68-E-01. 1968. ISBN 90-6144-001-7

2) **Veefkind, A., J.H. Blom and L.H.Th. Rietjens**
THEORETICAL AND EXPERIMENTAL INVESTIGATION OF A NON-EQUILIBRIUM PLASMA IN A MHD CHANNEL. Submitted to the Symposium on Magnetohydrodynamic Electrical Power Generation, Warsaw, Poland, 24-30 July, 1968.
TH-Report 68-E-02. 1968. ISBN 90-6144-002-5

3) **Boom, A.J.W. van den and J.H.A.M. Melis**
A COMPARISON OF SOME PROCESS PARAMETER ESTIMATING SCHEMES.
TH-Report 68-E-03. 1968. ISBN 90-6144-003-3

4) **Eykhoff, P., P.J.M. Ophey, J. Severs and J.O.M. Oome**
AN ELECTROLYTIC TANK FOR INSTRUCTIONAL PURPOSES REPRESENTING THE COMPLEX-FREQUENCY PLANE.
TH-Report 68-E-02. 1968. ISBN 90-6144-004-1

5) **Vermij, L. and J.E. Daalder**
ENERGY BALANCE OF FUSING SILVER WIRES SURROUNDED BY AIR.
TH-Report 68-E-05. 1968. ISBN 90-6144-005-X

6) **Houben, J.W.M.A. and P. Massee**
MHD POWER CONVERSION EMPLOYING LIQUID METALS.
TH-Report 69-E-06. 1969. ISBN 90-6144-006-8

7) **Heuvel, W.M.C. van den and W.F.J. Kersten**
VOLTAGE MEASUREMENT IN CURRENT ZERO INVESTIGATIONS.
TH-Report 69-E-07. 1969. ISBN 90-6144-007-6

8) **Vermij, L.**
SELECTED BIBLIOGRAPHY OF FUSES.
TH-Report 69-E-08. 1969. ISBN 90-6144-008-4

9) **Westenberg, J.Z.**
SOME IDENTIFICATION SCHEMES FOR NON-LINEAR NOISY PROCESSES.
TH-Report 69-E-09. 1969. ISBN 90-6144-009-2

10) **Koop, H.E.M., J. Dijk and E.J. Maanders**
ON CONICAL HORN ANTENNAS.
TH-Report 70-E-10. 1970. ISBN 90-6144-010-6

11) **Veefkind, A.**
NON-EQUILIBRIUM PHENOMENA IN A DISC-SHAPED MAGNETOHYDRODYNAMIC GENERATOR.
TH-Report 70-E-11. 1970. ISBN 90-6144-011-4

12) **Jansen, J.K.M., M.E.J. Jeuken and C.W. Lamerechtse**
THE SCALAR FEED.
TH-Report 70-E-12. 1969. ISBN 90-6144-012-2

13) **Teuling, D.J.A.**
ELECTRONIC IMAGE MOTION COMPENSATION IN A PORTABLE TELEVISION CAMERA.
TH-Report 70-E-13. 1970. ISBN 90-6144-013-0

EINDHOVEN UNIVERSITY OF TECHNOLOGY
THE NETHERLANDS
DEPARTMENT OF ELECTRICAL ENGINEERING

Reports:

14) **Lorencin, M.**
AUTOMATIC METEOR REFLECTIONS RECORDING EQUIPMENT.
TH-Report 70-E-14. 1970. ISBN 90-6144-014-9

15) **Smets, A.S.**
THE INSTRUMENTAL VARIABLE METHOD AND RELATED IDENTIFICATION SCHEMES.
TH-Report 70-E-15. 1970. ISBN 90-6144-015-7

16) **White, Jr., R.C.**
A SURVEY OF RANDOM METHODS FOR PARAMETER OPTIMIZATION.
TH-Report 70-E-16. 1971. ISBN 90-6144-016-5

17) **Talmon, J.L.**
APPROXIMATED GAUSS-MARKOV ESTIMATORS AND RELATED SCHEMES.
TH-Report 71-E-17. 1971. ISBN 90-6144-017-3

18) **Kalášek, V.**
MEASUREMENT OF TIME CONSTANTS ON CASCADE D.C. ARC IN NITROGEN.
TH-Report 71-E-18. 1971. ISBN 90-6144-018-1

19) **Hosselet, L.M.L.F.**
OZONBILDUNG MITTELS ELEKTRISCHER ENTLADUNGEN.
TH-Report 71-E-19. 1971. ISBN 90-6144-019-X

20) **Arts, M.G.J.**
ON THE INSTANTANEOUS MEASUREMENT OF BLOODFLOW BY ULTRASONIC MEANS.
TH-Report 71-E-20. 1971. ISBN 90-6144-020-3

21) **Roer, Th.G. van de**
NON-ISO THERMAL ANALYSIS OF CARRIER WAVES IN A SEMICONDUCTOR.
TH-Report 71-E-21. 1971. ISBN 90-6144-021-1

22) **Jeuken, P.J., C. Huber and C.E. Mulders**
SENSING INERTIAL ROTATION WITH TUNING FORKS.
TH-Report 71-E-22. 1971. ISBN 90-6144-022-X

23) **Dijk, J., J.M. Berends and E.J. Maanders**
APERTURE BLOCKAGE IN DUAL REFLECTOR ANTENNA SYSTEMS - A REVIEW.
TH-Report 71-E-23. 1971. ISBN 90-6144-023-8

24) **Kregting, J. and R.C. White, Jr.**
ADAPTIVE RANDOM SEARCH.
TH-Report 71-E-24. 1971. ISBN 90-6144-024-6

25) **Damen, A.A.H. and H.A.L. Piceni**
THE MULTIPLE DIPOLE MODEL OF THE VENTRICULAR DEPOLARISATION.
TH-Report 71-E-25. 1971. ISBN 90-6144-025-4

26) **Bremmer, H.**
A MATHEMATICAL THEORY CONNECTING SCATTERING AND DIFFRACTION PHENOMENA, INCLUDING BRAGG-TYPE INTERFERENCES.
TH-Report 71-E-26. 1971. ISBN 90-6144-026-2

27) **Bokhoven, W.M.G. van**
METHODS AND ASPECTS OF ACTIVE RC-FILTERS SYNTHESIS.
TH-Report 71-E-27. 1970. ISBN 90-6144-027-0

28) **Boeschoten, F.**
TWO FLUIDS MODEL REEXAMINED FOR A COLLISIONLESS PLASMA IN THE STATIONARY STATE.
TH-Report 72-E-28. 1972. ISBN 90-6144-028-9

EINDHOVEN UNIVERSITY OF TECHNOLOGY
THE NETHERLANDS
DEPARTMENT OF ELECTRICAL ENGINEERING

Reports:

29) REPORT ON THE CLOSED CYCLE MHD SPECIALIST MEETING. Working group of the joint ENEA/IAEA International MHD Liaison Group.
Eindhoven, The Netherlands, September 20-22, 1971. Edited by **L.H.Th. Rietjens.**
TH-Report 72-E-29. 1972. ISBN 90-6144-029-7

30) **Kessel, C.G.M. van and J.W.M.A. Houben**
LOSS MECHANISMS IN AN MHD GENERATOR.
TH-Report 72-E-30. 1972. ISBN 90-6144-030-0

31) **Veefkind, A.**
CONDUCTION GRIDS TO STABILIZE MHD GENERATOR PLASMAS AGAINST IONIZATION INSTABILITIES.
TH Report 72-E-31. 1972. ISBN 90-6144-031-9

32) **Daalder, J.E., and C.W.M. Vos**
DISTRIBUTION FUNCTIONS OF THE SPOT DIAMETER FOR SINGLE- AND MULTI-CATHODE DISCHARGES IN VACUUM.
TH-Report 73-E-32. 1973. ISBN 90-6144-032-7

33) **Daalder, J.E.**
JOULE HEATING AND DIAMETER OF THE CATHODE SPOT IN A VACUUM ARC.
TH-Report 73-E-33. 1973. ISBN 90-6144-033-5

34) **Huber, C.**
BEHAVIOUR OF THE SPINNING GYRO ROTOR.
TH-Report 73-E-34. 1973. ISBN 90-6144-034-3

35) **Bastian, C. et al.**
THE VACUUM ARC AS A FACILITY FOR RELEVANT EXPERIMENTS IN FUSION RESEARCH. Annual Report 1972. EURATOM-T.H.E. Group 'Rotating Plasma'.
TH-Report 73-E-35. 1973. ISBN 90-6144-035-1

36) **Blom, J.A.**
ANALYSIS OF PHYSIOLOGICAL SYSTEMS BY PARAMETER ESTIMATION TECHNIQUES.
TH-Report 73-E-36. 1973. ISBN 90-6144-036-X

37) **Cancelled**

38) **Andriessen, F.J., W. Boerman and I.F.E.M. Holtz**
CALCULATION OF RADIATION LOSSES IN CYLINDER SYMMETRIC HIGH PRESSURE DISCHARGES BY MEANS OF A DIGITAL COMPUTER.
TH-Report 73-E-38. 1973. ISBN 90-6144-038-6

39) **Dijk, J., C.T.W. van Diepenbeek, E.J. Maanders and L.F.G. Thurlings**
THE POLARIZATION LOSSES OF OFFSET ANTENNAS.
TH-Report 73-E-39. 1973. ISBN 90-6144-039-4

40) **Goes, W.P.**
SEPARATION OF SIGNALS DUE TO ARTERIAL AND VENOUS BLOOD FLOW IN THE DOPPLER SYSTEM THAT USES CONTINUOUS ULTRASOUND.
TH-Report 73-E-40. 1973. ISBN 90-6144-040-8

41) **Damen, A.A.H.**
A COMPARATIVE ANALYSIS OF SEVERAL MODELS OF THE VENTRICULAR DEPOLARIZATION; INTRODUCTION OF A STRING-MODEL.
TH-Report 73-E-41. 1973. ISBN 90-6144-041-6

EINDHOVEN UNIVERSITY OF TECHNOLOGY
THE NETHERLANDS
DEPARTMENT OF ELECTRICAL ENGINEERING

Reports:

42) **Dijk, G.H.M. van**
THEORY OF GYRO WITH ROTATING GIMBAL AND FLEXURAL PIVOTS.
TH-Report 73-E-42. 1973. ISBN 90-6144-042-4

43) **Breimer, A.J.**
ON THE IDENTIFICATION OF CONTINOUS LINEAR PROCESSES.
TH-Report 74-E-43. 1974. ISBN 90-6144-043-2

44) **Lier, M.C. van and R.H.J.M. Otten**
CAD OF MASKS AND WIRING.
TH-Report 74-E-44. 1974. ISBN 90-6144-044-0

45) **Bastian, C. et al.**
EXPERIMENTS WITH A LARGE SIZED HOLLOW CATHODE DISCHARDE FED WITH ARGON. Annual Report 1973. EURATOM-T.H.E. Group 'Rotating Plasma'.
TH-Report 74-E-45. 1974. ISBN 90-6144-045-9

46) **Roer, Th.G. van de**
ANALYTICAL SMALL-SIGNAL THEORY OF BARITT DIODES.
TH-Report 74-E-46. 1974. ISBN 90-6144-046-7

47) **Leliveld, W.H.**
THE DESIGN OF A MOCK CIRCULATION SYSTEM.
TH-Report 74-E-47. 1974. ISBN 90-6144-047-5

48) **Damen, A.A.H.**
SOME NOTES ON THE INVERSE PROBLEM IN ELECTRO CARDIOGRAPHY.
TH-Report 74-E-48. 1974. ISBN 90-6144-048-3

49) **Meeberg, L. van de**
A VITERBI DECODER.
TH-Report 74-E-49. 1974. ISBN 90-6144-049-1

50) **Poel, A.P.M. van der**
A COMPUTER SEARCH FOR GOOD CONVOLUTIONAL CODES.
TH-Report 74-E-50. 1974. ISBN 90-6144-050-5

51) **Sampic, G.**
THE BIT ERROR PROBABILITY AS A FUNCTION PATH REGISTER LENGTH IN THE VITERBI DECODER.
TH-Report 74-E-51. 1974. ISBN 90-6144-051-3

52) **Schalkwijk, J.P.M.**
CODING FOR A COMPUTER NETWORK.
TH-Report 74-E-52. 1974. ISBN 90-6144-052-1

53) **Stapper, M.**
MEASUREMENT OF THE INTENSITY OF PROGRESSIVE ULTRASONIC WAVES BY MEANS OF RAMAN-NATH DIFRACTION.
TH-Report 74-E-53. 1974. ISBN 90-6144-053-X

54) **Schalkwijk, J.P.M. and A.J. Vinck**
SYNDROME DECODING OF CONVOLUTIONAL CODES.
TH-Report 74-E-54. 1974. ISBN 90-6144-054-8

55) **Yakimov, A.**
FLUCTUATIONS IN IMPATT-DIODE OSCILLATORS WITH LOW Q-FACTORS.
TH-Report 74-E-55. 1974. ISBN 90-6144-055-6

EINDHOVEN UNIVERSITY OF TECHNOLOGY
THE NETHERLANDS
DEPARTMENT OF ELECTRICAL ENGINEERING

Reports:

56) **Plaats, J. van der**
ANALYSIS OF THREE CONDUCTOR COAXIAL SYSTEMS. Computer-aided determination of the frequency characteristics and the impulse and step response of a two-port consisting of a system of three coaxial conductors terminating in lumped impedances.
TH-Report 75-E-56. 1975. ISBN 90-6144-056-4

57) **Kalken, P.J.H. and C. Kooy**
RAY-OPTICAL ANALYSIS OF A TWO DIMENSIONAL APERTURE RADIATION PROBLEM.
TH-Report 75-E-57. 1975. ISBN 90-6144-057-2

58) **Schalkwijk, J.P.M., A.J. Vinck and L.J.A.E. Rust**
ANALYSIS AND SIMULATION OF A SYNDROME DECODER FOR A CONSTRAINT LENGTH k = 5, RATE R = ½ BINARY CONVOLUTIONAL CODE.
TH-Report 75-E-58. 1975. ISBN 90-6144-058-0.

59) **Boeschoten, F. et al.**
EXPERIMENTS WITH A LARGE SIZED HOLLOW CATHODE DISCHARGE FED WITH ARGON, II. Annual Report 1974. EURATOM-T.H.E. Group 'Rotating Plasma'.
TH-Report 75-E-59. 1975. ISBN 90-6144-059-9

60) **Maanders, E.J.**
SOME ASPECTS OF GROUND STATION ANTENNAS FOR SATELLITE COMMUNICATION.
TH-Report 75-E-60. 1975. ISBN 90-6144-060-2

61) **Mawira, A. and J. Dijk**
DEPOLARIZATION BY RAIN: Some Related Thermal Emission Considerations.
TH-Report 75-E-61. 1975. ISBN 90-6144-061-0

62) **Safak, M.**
CALCULATION OF RADIATION PATTERNS OF REFLECTOR ANTENNAS BY HIGH-FREQUENCY ASYMPTOTIC TECHNIQUES.
TH-Report 76-E-62. 1976. ISBN 90-6144-062-9

63) **Schalkwijk, J.P.M. and A.J. Vinck**
SOFT DECISION SYNDROME DECODING.
TH-Report 76-E-63. 1976. ISBN 90-6144-063-7

64) **Damen, A.A.H.**
EPICARDIAL POTENTIALS DERIVED FROM SKIN POTENTIAL MEASUREMENTS.
TH-Report 76-E-64. 1976. ISBN 90-6144-064-5

65) **Bakhuizen, A.J.C. and R. de Boer**
ON THE CALCULATION OF PERMEANCES AND FORCES BETWEEN DOUBLY SLOTTED STRUCTURES.
TH-Report 76-E-65. 1976. ISBN 90-6144-065-3

66) **Geutjes, A.J.**
A NUMERICAL MODEL TO EVALUATE THE BEHAVIOUR OF A REGENERATIVE HEAT EXCHANGER AT HIGH TEMPERATURE.
TH-Report 76-E-66. 1976. ISBN 90-6144-066-1

67) **Boeschoten, F. et al.**
EXPERIMENTS WITH A LARGE SIZED HOLLOW CATHODE DISCHARGE, III; concluding work Jan. 1975 to June 1976 of the EURATOM-THE Group 'Rotating Plasma'.
TH-Report 76-E-67. 1976. ISBN 90-6144-067-X

68) **Cancelled.**

EINDHOVEN UNIVERSITY OF TECHNOLOGY
THE NETHERLANDS
DEPARTMENT OF ELECTRICAL ENGINEERING

Reports:

69) Merck, W.F.H. and A.F.C. Sens
THOMSON SCATTERING MEASUREMENTS ON A HOLLOW CATHODE DISCHARGE.
TH-Report 76-E-69. 1976. ISBN 90-6144-069-6

70) Jongbloed, A.A.
STATISTICAL REGRESSION AND DISPERSION RATIOS IN NONLINEAR SYSTEM IDENTIFICATION.
TH-Report 77-E-70. 1977. ISBN 90-6144-070-X

71) Barrett, J.F.
BIBLIOGRAPHY ON VOLTERRA SERIES HERMITE FUNCTIONAL EXPANSIONS AND RELATED SUBJECTS.
TH-Report 77-E-71. 1977. ISBN 90-6144-071-8

72) Boeschoten, F. and R. Komen
ON THE POSSIBILITY TO SEPARATE ISOTOPES BY MEANS OF A ROTATING PLASMA COLUMN: Isotope separation with a hollow cathode discharge.
TH-Report 77-E-72. 1977. ISBN 90-6144-072-6

73) Schalkwijk, J.P.M., A.J. Vinck and K.A. Post
SYNDROME DECODING OF BINARY RATE-k/n CONVOLUTIONAL CODES.
TH-Report 77-E-73. 1977. ISBN 90-6144-073-4

74) Dijk, J., E.J. Maanders and J.M.J. Oostvogels
AN ANTENNA MOUNT FOR TRACKING GEOSTATIONARY SATELLITES.
TH-Report 77-E-74. 1977. ISBN 90-6144-074-2

75) Vinck, A.J., J.G. van Wijk and A.J.P. de Paepe
A NOTE ON THE FREE DISTANCE FOR CONVOLUTIONAL CODES.
TH-Report 77-E-75. 1977. ISBN 90-6144-075-0

76) Daalder, J.E.
RADIAL HEAT FLOW IN TWO COAXIAL CYLINDRICAL DISKS.
TH-Report 77-E-76. 1977. ISBN 90-6144-076-9

77) Barrett, J.F.
ON SYSTEMS DEFINED BY IMPLICIT ANALYTIC NONLINEAR FUNCTIONAL EQUATIONS.
TH-Report 77-E-77. 1977. ISBN 90-6144-077-7

78) Jansen, J. and J.F. Barrett
ON THE THEORY OF MAXIMUM LIKELIHOOD ESTIMATION OF STRUCTURAL RELATIONS. Part 1: One dimensional case.
TH-Report 78-E-78. 1977. ISBN 90-6144-078-5

79) Borghi, C.A., A.F.C. Sens, A. Veefkind and L.H.Th. Rietjens
EXPERIMENTAL INVESTIGATION ON THE DISCHARGE STRUCTURE IN A NOBLE GAS MHD GENERATOR.
TH-Report 78-E-79. 1978. ISBN 90-6144-079-3

80) Bergmans, T.
EQUALIZATION OF A COAXIAL CABLE FOR DIGITAL TRANSMISSION: Computer-optimized location of poles and zeros of a constant-resistance network to equalize a coaxial cable 1.2/4.4 for high-speed digital transmission (140 Mb/s).
TH-Report 78-E-80. 1978. ISBN 90-6144-080-7

EINDHOVEN UNIVERSITY OF TECHNOLOGY
THE NETHERLANDS
DEPARTMENT OF ELECTRICAL ENGINEERING

Reports:

81) Kam, J.J. van der and A.A.H. Damen
OBSERVABILITY OF ELECTRICAL HEART ACTIVITY STUDIED WITH THE SINGULAR VALUE DECOMPOSITION
TH-Report 78-E-81. 1978. ISBN 90-6144-081-5

82) Jansen, J. and J.F. Barrett
ON THE THEORY OF MAXIMUM LIKELIHOOD ESTIMATION OF STRUCTURAL RELATIONS. Part 2: Multi-dimensional case.
TH-Report 78-E-82. 1978. ISBN 90-6144-082-3

83) Etten, W. van and E. de Jong
OPTIMUM TAPPED DELAY LINES FOR THE EQUALIZATION OF MULTIPLE CHANNEL SYSTEMS.
TH-Report 78-E-83. 1978. ISBN 90-6144-083-1

84) Vinck, A.J.
MAXIMUM LIKELIHOOD SYNDROME DECODING OF LINEAR BLOCK CODES.
TH-Report 78-E-84. 1978. ISBN 90-6144-084-X

85) Spruit, W.P.
A DIGITAL LOW FREQUENCY SPECTRUM ANALYZER, USING A PROGRAMMABLE POCKET CALCULATOR.
TH-Report 78-E-85. 1978. ISBN 90-6144-085-8

86) Beneken, J.E.W. et al.
TREND PREDICTION AS A BASIS FOR OPTIMAL THERAPY.
TH-Report 78-E-86. 1978. ISBN 90-6144-086-6

87) Geus, C.A.M. and J. Dijk
CALCULATION OF APERTURE AND FAR-FIELD DISTRIBUTION FROM MEASUREMENTS IN THE FRESNEL ZONE OF LARGE REFLECTOR ANTENNAS.
TH-Report 78-E-87. 1978. ISBN 90-6144-087-4

88) Hajdasinski, A.K.
THE GAUSS-MARKOV APPROXIMATED SCHEME FOR IDENTIFICATION OF MULTIVARIABLE DYNAMICAL SYSTEMS VIA THE REALIZATION THEORY. An Explicit Approach.
TH-Report 78-E-88. 1978. ISBN 90-6144-088-2

89) Niederlinski, A.
THE GLOBAL ERROR APPROACH TO THE CONVERGENCE OF CLOSED-LOOP IDENTIFICATION, SELF-TUNING REGULATORS AND SELF-TUNING PREDICTORS.
TH-Report 78-E-89. 1978. ISBN 90-6144-089-0

90) Vinck, A.J. and A.J.P. de Paepe
REDUCING THE NUMBER OF COMPUTATIONS IN STACK DECODING OF CONVOLUTIONAL CODES BY EXPLOITING SYMMETRIES OF THE ENCODER.
TH-Report 78-E-90. 1978. ISBN 90-6144-090-4